Climate and climate change in a radiative-convective equilibrium version of ECHAM6

D. Popke,[1] B. Stevens,[1] and A. Voigt[1]

Received 31 July 2012; revised 19 November 2012; accepted 10 December 2012; published 28 January 2013.

[1] A radiative-convective equilibrium (RCE) configuration of a comprehensive atmospheric general circulation model, ECHAM6, is coupled to a mixed-layer ocean for the purpose of advancing understanding of climate and climate change. This configuration differs from a standard configuration only through the removal of land-surface processes, spatial gradients in solar insolation, and the effects of rotation. Nonetheless, the model produces a climate that resembles the tropical climate in a control simulation of Earth's atmosphere. In the RCE configuration, regional inhomogeneities in surface temperature develop. These inhomogeneities are transient in time but sufficiently long-lived to establish large-scale overturning circulations with a distribution similar to the preindustrial tropics in the standard configuration. The vertical structure of the atmosphere, including profiles of clouds and condensate conditioned on the strength of overturning, also resembles those produced by a control simulation of Earth's tropical atmosphere. The equilibrium climate sensitivity of the RCE atmosphere can explain 50% of the global climate sensitivity of a realistic configuration of ECHAM6. Part of the difference is attributed to the lack of polar amplification in RCE. The remainder appears to be related to a less positive cloud shortwave feedback, which results from an increase in low cloudiness with increasing surface temperatures in the RCE configuration. The RCE configuration shows an increase of climate sensitivity in a warmer climate. The increase in climate sensitivity scales with the degree to which the upper-troposphere temperature departs from a moist adiabat.

Citation: Popke, D., B. Stevens, and A. Voigt (2013), Climate and climate change in a radiative-convective equilibrium version of ECHAM6, *J. Adv. Model. Earth Syst.*, *5*, 1–14, doi:10.1029/2012MS000191.

1. Introduction

[2] A tenet of our understanding of climate change is that models of the Earth system respond similarly to a perturbation in greenhouse gases, such as CO_2, irrespective of their details. *Bony et al.* [2011] point out that the enduring insights in the Charney report [*Charney et al.*, 1979], and its estimate of the expected temperature response $\Delta T_{2\times}$ associated with a doubling of CO_2, can be attributed to the report's ability to identify robust behavior across a hierarchy of models and connect this behavior with physical principles. Understanding of climate change will not advance if it is based on authority claims by incomprehensibly comprehensive models. Rather, understanding develops by working through a hierarchy of models, and model configurations, to connect robust behavior of the most comprehensive models to basic physical principles, laws, or facts [e.g., *Held*, 2005; *Bony et al.*, 2011].

[3] The concept of radiative-convective equilibrium (RCE) has long had an important place in the hierarchy of models that we use to connect physical laws to the complex behavior of the Earth system. In criticizing the results of *Callendar*'s [1938] initial studies of the effect of CO_2 on climate, Sir George Simpson presciently noted that any theory of climate change must consider how heat is transferred into the atmosphere by convection. It took nearly 30 years until this basic insight was addressed by *Manabe and Strickler* [1964] and *Manabe and Wetherald* [1967], who constructed the first satisfactory theory of the relationship between radiative forcing and surface temperature. This work required the development of one of the first parameterizations of deep moist convection and formed the basis for what we today call RCE. The idea that, to a useful degree of approximation, the atmosphere is well described by RCE revolutionized understanding of the greenhouse effect and forever established RCE as a staple of the climate change diet.

[4] The tropics, equatorward of 30°, absorb, on average, about 400 W m^{-2} of solar radiation, of which less

[1]Max Planck Institute for Meteorology, The Atmosphere in the Earth System, Hamburg, Germany.

1942-2466/13/2012MS000191

than 20% is exported to the extratropics. The remainder is balanced through the emission of longwave radiation to space, which cools the atmosphere and begets convection. The enthalpy of vaporization released into the tropical atmosphere as a result of net condensation (equivalently surface precipitation) is about twice as large as the amount of energy exported to the extratropics per unit time. All of which suggests that RCE, which has come to be seen as a good paradigm for the climate system as a whole, is an especially good paradigm for the tropical atmosphere, notwithstanding complications associated with large-scale circulations, which develop in response to inhomogeneous surface conditions and interactions with the extratropics. Thus, in addition to the question of climate change more generally, the relevance of the RCE paradigm to tropical circulations and studies of deep convection makes it broadly interesting.

[5] As greater computational resources became available, the application of the RCE paradigm progressively evolved from the earliest one-dimensional models to cloud-resolving models, initially in two-dimensional configurations [*Held et al*., 1993]. By explicitly representing convective-scale circulations, such studies were able to relax many of the artificial and potentially limiting assumptions, such as the need to specify (or very crudely parameterize) the distribution of clouds and water vapor (see *Ramanathan and Coakley* [1978] for a review). Subsequently, cloud-resolving models and even large-eddy simulation approaches [*Romps*, 2011] have increasingly come to be used to study a wide number of issues in the context of RCE, including controls on the hydrological cycle and precipitation extremes [*Romps*, 2011; *Muller et al*., 2011], the distribution of convective mass fluxes [*Tompkins and Craig*, 1998], scaling laws for moist convection [*Robe and Emanuel*, 1996], aerosol-cloud interactions [*Grabowski*, 2003; *van den Heever et al*., 2011], entropy budgets [*Pauluis and Held*, 2002], and factors controlling convective organization [*Bretherton et al*., 2005]. Contemporaneously, very simple RCE models continue to be used to inform the study of fundamental questions in planetary atmospheres, such as the question of a runaway greenhouse effect [e.g., *Sugiyama et al*., 2005].

[6] In this study, RCE is investigated with a comprehensive atmospheric general circulation model (GCM), ECHAM6, coupled to a mixed-layer ocean. One motivation for doing so is purely methodological, to fill a gap in the model hierarchy and better link high-resolution modeling efforts on the one hand and comprehensive modeling of the Earth system on the other. There is surprisingly little precedent for such an approach. Only one other study that we are aware of [*Held et al*., 2007] attempts something similar, but the behavior of the GCM column physics in a Cartesian geometry with fixed sea surface temperatures (SSTs) is designed as an analog to cloud-resolving simulations. A slightly different approach is taken here, as a comprehensive GCM is used to study the behavior of the Earth's atmosphere under spatially uniform solar insolation, in the absence of rotation, as a function of atmospheric CO_2 concentrations. In essence, the problem posed by *Manabe and Wetherald* [1967] is revisited with a full physics GCM, which allows clouds and water vapor to develop consistently with the model's circulations. This allows us to address a second motivation, which is to establish whether the behavior of the GCM in this configuration resembles in any way the behavior of simple models of climate change on the one hand and the behavior of the full fledged GCM as applied to more realistic boundary conditions on the other hand. To the extent it does, it contributes to longstanding efforts to extend the model hierarchy in ways that enable the identification and rationalization of robust behavior of complex systems to simple physical principles, what one might call understanding [*Held*, 2005; *Medeiros et al*., 2008; *Bony et al*., 2011].

[7] The remainder of this study is organized as follows: In section 2, the model configuration and experimental methodology are described. In section 3, the mean preindustrial climate in RCE is compared with the tropical climate as simulated by the Earth-system configuration of the model, which naturally includes additional processes associated with the land-surface and ocean dynamics. The response of the model to a fourfold increase and reduction in greenhouse gas concentrations is presented in section 4, wherein a particular emphasis is placed on linking the model behavior to robust aspects of our present understanding of climate change. Because deep moist convection (hereafter simply referred to as deep convection) plays such an important role in the RCE paradigm, simulations are carried out with two variants of the ECHAM6 convection scheme, which have been shown in the previous studies to span a wide range in behavior, thereby helping to bound the response of the model to plausible representations of deep convection. Conclusions are presented in section 5.

2. Method and Model

[8] RCE is explored using the default, T63L47, version of ECHAM6 coupled to a mixed-layer ocean of 50 m depth. This version of ECHAM6 is identical, subject to modifications discussed below, to the LR (low resolution) version of the model as described by B. Stevens et al. (The atmospheric component of the MPI-M Earth: ECHAM6, submitted to *Journal of Advances in Modeling Earth Systems*, 2012), which served as the atmospheric component of the MPI-ESM (Max Planck Institute for Meteorology Earth System Model) (M. Giorgetta et al., Climate change from 1850 to 2100 in MPI-ESM CMIP5 simulations, *Journal of Advances in Modeling Earth Systems*, in preparation, 2012), used in the fifth phase of the coupled model intercomparison project (CMIP5) [*Taylor et al*., 2012]. The tuning constants used in the MPI-ESM [e.g., *Mauritsen et al*., 2012] are the same as used for the RCE studies. Being a comprehensive atmospheric GCM, ECHAM6 includes a full suite of parameterized physics, including parameterized moist convection, a cloud scheme based on a critical relative humidity (RH), cloud microphysics, and advanced treatments of radiative transfer, as described more fully by Stevens et al. (submitted manuscript, 2012). Running it for many tens of

simulated years at T63L47 resolution for the purposes of representing RCE represents a considerable investment of computational resources, for what is usually thought of as a simple problem. Below we describe how the model was configured to solve for RCE, and the experiments and analysis methods.

2.1. Configuring ECHAM6 for RCE

[9] To simulate RCE with ECHAM6 required boundary conditions to be homogenized. This is performed by representing the lower boundary as a uniform mixed-layer ocean of 50 m depth, setting the rotation rate to zero, adjusting climatologies of trace-gases and aerosols so that their longitudinal and latitudinal dependencies vanish, and adjusting the incoming solar insolation so that every model grid point sees the same incident radiation. In some cases, this implies a change in model parameters, as some parameterizations depend on the boundary conditions being homogenized. These points are elaborated upon below.

[10] In ECHAM6, the incident solar irradiance at the top of the atmosphere is given by

$$F(\lambda,\phi,t)=I_0\left(\frac{d_{se0}}{d_{se}(t)}\right)^2\mu_0(\lambda,\phi,t), \tag{1}$$

where I_0 = 1361 W m^{-2} is the total solar irradiance, $d_{se}(t)$ is the time-varying distance between Earth and Sun following Earth's orbit, d_{se0} is its annual average, μ_0 is the cosine of the solar zenith angle, and $\{\lambda,\phi\}$ are the spatial coordinates, denoting longitude and latitude, respectively. For RCE, the above expression is reformulated, such that

$$\tilde{F}(\lambda,\phi,t)=\tilde{I}_0\mu_0(0,0,t), \tag{2}$$

thus preserving the diurnal cycle but removing any dependence of the incident solar irradiance on longitude or latitude. An effective, smaller, total solar irradiance, $\tilde{I}_0$=1069.3 W m^{-2} is introduced in equation (2), so that when averaged over the diurnal cycle $\tilde{F}$ equals the global and annual average of F, which following equation (1) has a value of 340.3 W m^{-2}. Except for CO_2, which is varied in the experiments, the input gas climatologies are set to preindustrial conditions: methane and nitrous oxide volume mixing ratios were set to values of 650 and 270 ppbv, respectively, and chlorofluorocarbon concentrations are set to zero. Following the aqua-planet protocol, aerosol concentrations were also set to zero. The model ozone climatology was everywhere set to its preindustrial value at $\{\lambda,\phi\}=\{0,0\}$, i.e., a tropical profile as shown in Figure 1. Simulations were also performed without a diurnal cycle and with the mixed-layer ocean depth reduced from 50 to 25 m. However, because those simulations did not differ from the ones presented here, their results are not discussed further.

[11] In ECHAM6, the formulation of a minimum depth for the stable boundary layer depends on the Coriolis parameter and must be adjusted in the RCE configuration. This limitation is simply removed from the calculation of the boundary layer depth, consistent with the boundary layer behavior at the equator in ECHAM6. Additionally, sea-ice formation was inhibited, although temperatures were never approached where this would have been an issue; the mass of the atmosphere is increased to compensate for the lack of mountains and ensure that the mean sea-level pressure in the model has a value of 1013.25 hPa; and the surface albedo is given a fixed value of 0.07, corresponding to the insolation weighted globally averaged value. At last, we note that ECHAM6 has a spectral dynamical core, but physics are performed on a transform grid in latitude-longitude space. The latter is not isotropic but still very symmetric. Symmetry is broken by noise in the initial data. The effect of grid anisotropy was explored in the analysis but not found to be important.

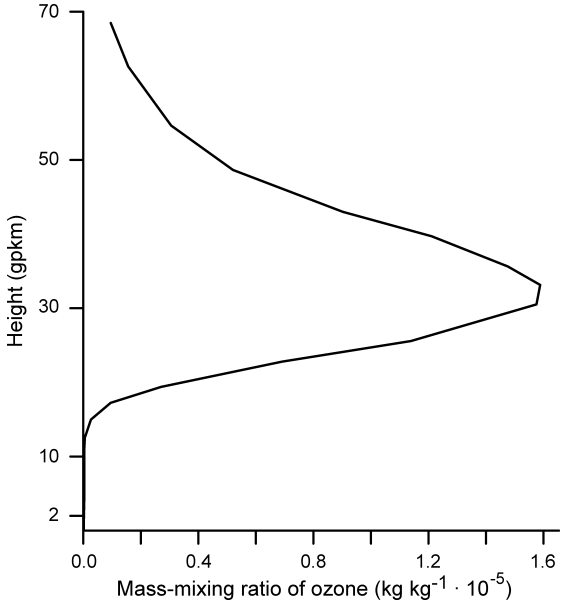

Figure 1. The equatorial vertical ozone profile that is employed in each column of the RCE simulations.

2.2. Experiments and Analysis Methods

[12] Three pairs of simulations of RCE are presented. The three pairs differ from one another only in their specified CO_2 concentrations, which vary from preindustrial values of 278 ppmv to values fourfold larger and smaller. Members of a simulation pair differ in their representation of deep convection. Because deep convection plays such an important role in RCE, simulations were performed with both the default ECHAM6 configurations, which employs Nordeng's 1994 modification to the *Tiedtke* [1989] scheme and the Tiedtke scheme itself. Only the representation of deep convection is affected by Nordeng's modifications, whereas shallow and midlevel convection are represented identically in both schemes. Although Nordeng's modifications are relatively minor, as implemented they have a large impact. For instance, ECHAM6 well represents

tropical intraseasonal variability, but when run with Tiedtke, there is no sign of eastward propagating intraseasonal variability [*Crueger et al.*, 2012]. Likewise, ECHAM6 produces a single, near-equatorial Intertropical Convergence Zone (ITCZ), but ECHAM6 run with Tiedtke produces a clear double ITCZ (B. Möbis and B. Stevens, Factors controlling the position of the ITCZ on an Aquaplanet, submitted to *Journal of Advances in Modeling Earth Systems*, 2012). The main difference between the schemes is that Nordeng's modifications lead to more mixing, which couples deep convection more strongly to the amount of moisture in the lower middle troposphere and leads to a more unstable atmosphere for a given value of boundary layer moist static energy (cf., Möbis and Stevens, submitted manuscript, 2012, for a thorough discussion of these issues). Hereafter, to distinguish between RCE simulations performed using standard ECHAM6 (i.e., with Nordeng's modifications) and ECHAM6-Tiedtke, experiments are referred to as *Nordeng* or *Tiedtke*, respectively. Each simulation is run for at least 40 years, and the analysis is performed over the last 30 years, as summarized in Table 1.

[13] In addition, 20 years of monthly averaged data from the 1000 year long piControl simulation, performed using the MPI-ESM-LR (Giorgetta et al., in preparation, 2012), and 20 years of data from the two mixed-layer ocean experiments based on ECHAM6-LR are analyzed for the purpose of comparison between the RCE experiments and the tropical climate of the MPI-ESM. Our analysis of these more realistic simulations focuses on the tropical oceans, defined based on a consideration of the mass stream function, to be the regions equatorward of 30°.

[14] In section 3.3, the mean climate state of the atmosphere is conditionally analyzed based on dynamic regimes [cf., *Bony et al.*, 2004]. The vertical velocity $\omega(p,\lambda,\phi,t)$, expressed in hPa d^{-1}, is used as a proxy of large-scale motion corresponding to positive values in large-scale subsiding and negative values in ascending regions. For this analysis, the local value of the mass-weighted average of $\omega(p,\lambda,\phi,t)$ from 925 to 200 hPa, i.e., $\overline{\omega}(\lambda,\phi,t)$, defines a regime so that the conditional average, $\langle g\rangle_{\overline{\omega}_i}$ of a generic field $g(\lambda,\phi,t)$ can be calculated as follows:

$$\langle g\rangle_{\overline{\omega}_i}=\frac{1}{\Omega_i}\int_{t_0}^{t_1}\int_{0}^{2\pi}\int_{-\pi/2}^{\pi/2} g\delta(\overline{\omega}-\overline{\omega}_i)\cos\phi\,\mathrm{d}\phi\,\mathrm{d}\lambda\,\mathrm{d}t', \qquad (3)$$

where $\delta(\omega-\omega')$ is the discrete dirac-delta function; t_0 and t_1 denote the start and end of the analysis period, respectively; and Ω_i gives the area weighting. On Earth, regimes are quasi-stationary and distributed spatially, in which case monthly averaged data can be used for this analysis [cf., *Bony et al.*, 2004]. For RCE, the domain is homogeneous so that one expects long-term averages of $\overline{\omega}$ to vanish. However, if $\overline{\omega}$ varies too rapidly, it does not make sense to speak of regimes, as the timescale of convective adjustment should be shorter than the timescale over which $\overline{\omega}$ varies for the local flow to adjust to the large-scale circulations, and thus expresses the idea of a regime. As discussed in section 3.1, convective areas are relatively long-lived in the simulations with the mixed-layer ocean. The integral timescale, $\tau_{\overline{\omega}}$, for these features can be estimated by regressing a function of the form $\exp(-\tau/\tau_{\overline{\omega}})$ against the horizontally averaged autocorrelation functions derived at all grid boxes with time lag τ. Doing so yields an estimate of $\tau_{\overline{\omega}}$. For Nordeng, $\tau_{\overline{\omega}}=4.4$ days and for Tiedtke, $\tau_{\overline{\omega}}=6.3$ days, based on which weekly data are used for the purpose of regime compositing. The use of a data averaged over a period slightly longer than the integral timescale implies that the full variability of $\overline{\omega}$ is not sampled but ensures that independent events are sampled.

3. Climate of the RCE Model

[15] In this section, we describe the mean and some conditionally averaged aspects of the climate that develops for both the preindustrial Nordeng and Tiedtke RCE simulations and compare them with the mean preindustrial tropical climate, as represented by the piControl of the MPI-ESM-LR. The three simulations are referred to as Nordeng, Tiedtke, and piControl, respectively. The

Table 1. Overview of Simulations[a]

Simulation	Simulation Length (Years)	Equilibrium Average (Years)	Weekly Average (Years)
		Nordeng and Tiedtke	
$\frac{1}{4}\times CO_2$	40	11–40	38–40
$1\times CO_2$	60	31–60	58–60
$4\times CO_2$	40	11–40	38–40
		piControl	
$1\times CO_2$	1000	Last 20 years	
		ECHAM6 (MLO)	
$1\times CO_2$	30	1920–1949	
$4\times CO_2$	30	1920–1949	

[a]MLO refers to mixed-layer ocean simulations.

main question to be answered is to what extent the climates of these differing configurations are similar.

3.1. Phenomenology

[16] At the outset, it was not clear to the authors whether or not ECHAM6 would be able to simulate a realistic RCE climate whatsoever. How would surface winds develop, would the inhomogeneous latitude-longitude grid cause the convection to lock at particular latitudes, and would the climate stabilize anywhere near present-day temperatures? To develop a feel for the types of circulations that develop, which are averaged over in the subsequent analysis, a sequence of four monthly snapshots, showing cloud cover, surface winds, and precipitation is presented in Figure 2. Large organized convective clusters are evident; they range in size from a few degrees to scales commensurate with present-day continents. In the first displayed month, one convective system stretches over a large portion of the eastern hemisphere. In subsequent months, this large-scale structure breaks apart, and new differently sized clusters develop. Figure 2 shows no evidence of convection being influenced by grid inhomogeneities, as it may occur in all regions of the Earth and does not, for instance, lock over the polar points. The occurrence of convection is associated with variable SSTs. The difference between the warmest and the coldest surface temperatures is about 6 K for Nordeng and 9 K for Tiedtke; in this way, our simulations differ from the previous simulations of RCE with a comprehensive GCM in which SSTs were held fixed [*Held et al.*, 2007].

[17] The organized nature of the convective systems is illustrated with the help of a Hovmöller diagram of $\overline{\omega}(\lambda, 0, t)$ (Figure 3). A clear distinction in the variability of convection between Nordeng and Tiedtke is visible, with Nordeng distributing the convection more homogeneously in time-longitude space than Tiedtke. Larger areas of weaker subsidence (negative vertical velocity) persist in Tiedtke than in Nordeng, as do very long-lived convective systems, some of which are coherent

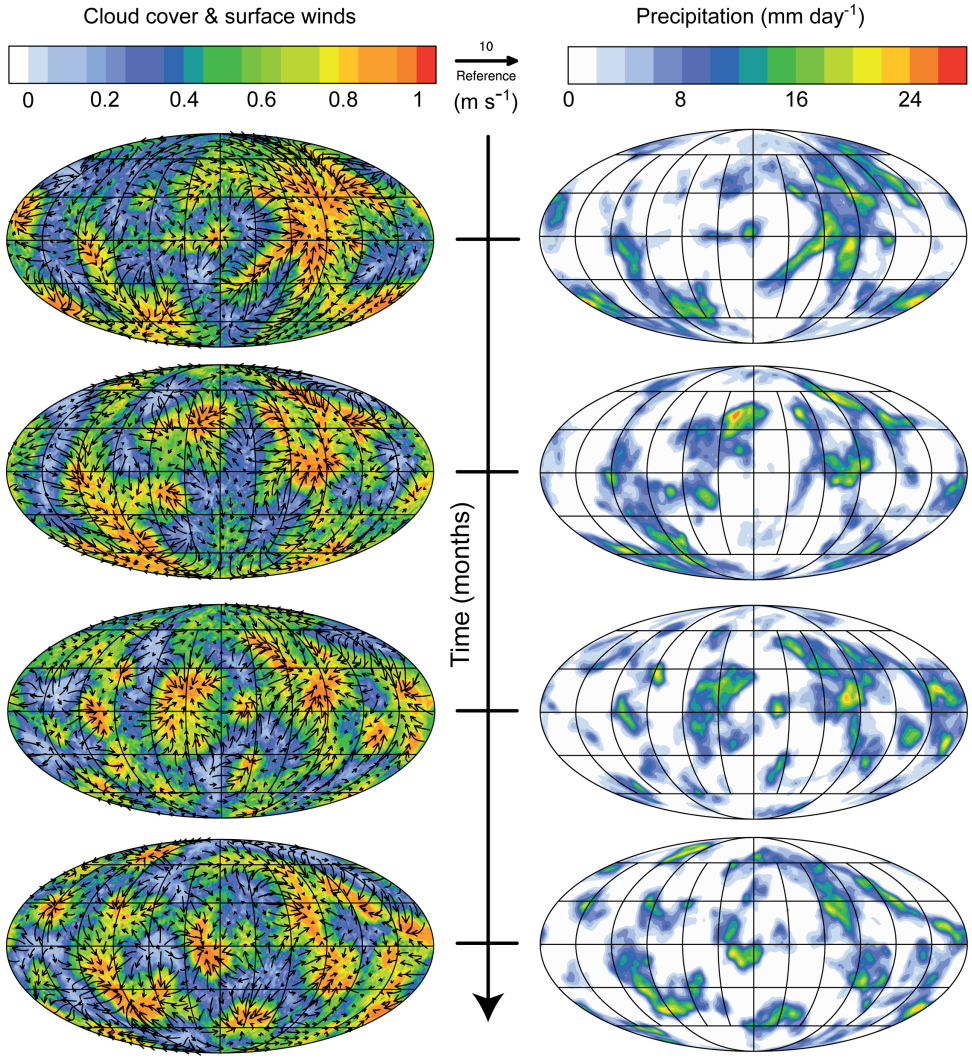

Figure 2. Four snapshots of consecutive monthly averaged (left) cloud cover in contours and surface winds as vectors and (right) precipitation. The RCE model is used with the Nordeng convection scheme.

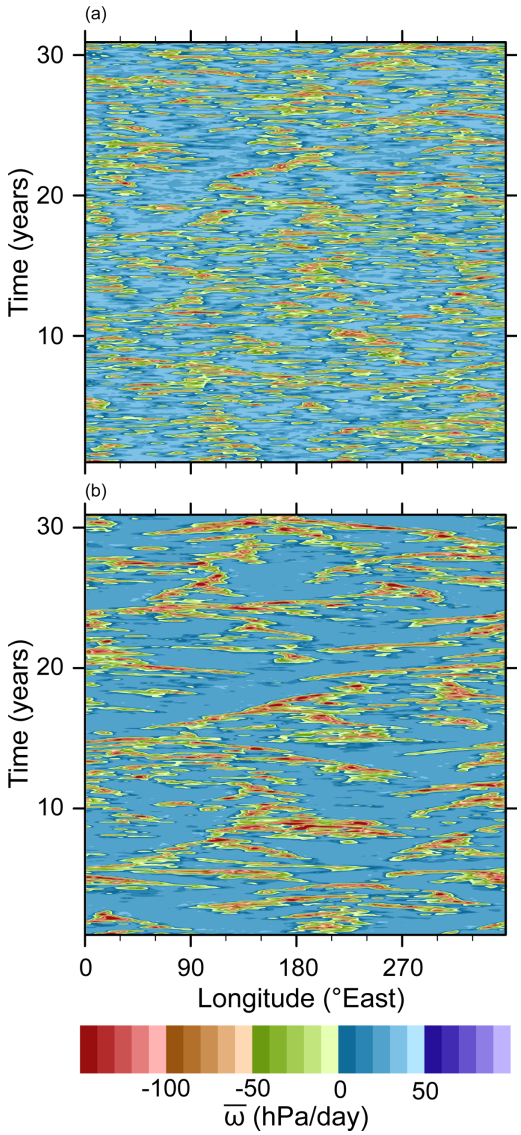

Figure 3. Hovmöller diagram of the vertical velocity mass-weighted averaged from 925 to 200 hPa at the equator using monthly data from the RCE model with the (a) Nordeng and (b) Tiedtke convection scheme. Variability of convective activity over 30 years in equilibrium is shown.

for periods of many years, which propagate very slowly in both eastward and westward directions. Smaller, more rapidly propagating systems are also evident; as to be expected, a preferred direction of propagation is not evident. Although only diagrams for the equator ($\phi = 0$) are shown, Hovmöller diagrams created for different latitudes demonstrate the same features. Given the longevity of the regions of upwelling and downwelling motions, it makes sense to think of large-scale dynamical regimes in these simulations, which motivates the analysis in section 3.3.

3.2. Mean Climate

[18] Notwithstanding different patterns of variability, the preindustrial RCE climates of Nordeng and Tiedtke are similar to the preindustrial tropical climate. Globally averaged surface temperatures are within a few degrees of the average tropical surface temperature in piControl (Table 2). Tiedtke is slightly warmer than Nordeng, but this may simply reflect the different effect of how the clouds were tuned when developing the MPI-ESM-LR. Monthly mean surface winds in the RCE model exhibit the same order of magnitude as in the more realistic piControl. Additionally, the equilibrium mean precipitation of Nordeng with 4.1 mm d^{-1} and Tiedtke with 4.6 mm d^{-1} compare well with the tropical average over the ocean in the piControl of 3.9 mm d^{-1}. Differences among the simulations are, in the sense, expected if the intensity of the hydrological cycle increases with warming [*Andrews et al.*, 2009], albeit larger. Nonetheless it is surprising, and perhaps fortuitous, that the mean temperatures of the preindustrial RCE simulations are so similar to those of the piControl. In piControl, the tropics are driven by higher values of the solar irradiance than the globally averaged values used to drive the RCE simulations (400 W m^{-2} for piControl tropics versus 340.3 W m^{-2} for the RCE simulations), but the difference is largely exported to the extratropics so that the temperatures are broadly similar (Table 2).

[19] The vertical temperature, RH, cloud fraction, and condensate also closely resemble the mean tropical state of the piControl simulation (Figure 4). Because the surface temperatures in the RCE simulations are similar to those of the piControl, and the tropical atmosphere thermal structure is determined by the lapse rate in the regions of convection, it stands to reason that the vertical temperature profile would also be similar. However, to the extent that the mean distribution of water vapor and clouds reflect the degree of large-scale organization in the tropics, it is not obvious that the RCE profiles of these quantities would so closely represent those of the piControl tropics. The RCE RH profiles share the double peak structure, with near-surface (900 hPa) and upper-troposphere (150 hPa) RH maxima of 80% and 70%, respectively, and a dry mid-troposphere (500 hPa) where RH minimizes with values

Table 2. Mean Properties of the RCE Model[a] at Stationarity (Using the Nordeng or Tiedtke Convection Scheme) and piControl

Experiment	SST (K)	TOA Albedo	Net Shortwave (W m^{-2})	OLR (W m^{-2})
Nordeng	300.1	0.20	272.5	272.9
Tiedtke	302.4	0.19	276.5	277.4
piControl, ocean tropics	298.4	0.21	314.7	260.7

[a]Imbalance of top of atmosphere (TOA) fluxes for Tiedtke and Nordeng is indicative of lack of perfect energy conservation in ECHAM.

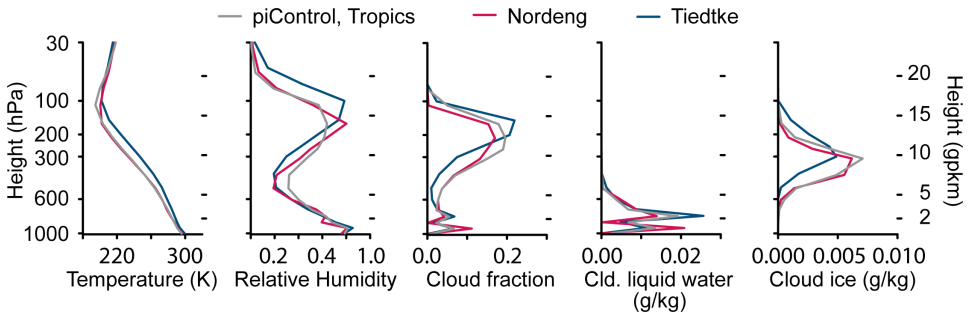

Figure 4. Comparison of RCE model (using either the Nordeng or Tiedtke scheme) vertical profiles with piControl vertical profiles of equilibrium mean temperature, RH, cloud fraction, cloud liquid water, and cloud ice calculated from monthly averaged data over 30 years in equilibrium, with preindustrial concentrations of CO_2. For the piControl profiles, only 20 years of monthly means are used, considering only tropical ocean grid points.

near 30%. Both Tiedtke and Nordeng are somewhat drier in the middle troposphere and somewhat moister in the upper troposphere than piControl. The somewhat drier atmosphere is consistent with slightly elevated values of outgoing longwave radiation (OLR) as compared with the piControl (Table 2). The basic structure of the condensate distribution is also similar. Tiedtke, Nordeng, and the piControl have a three layer structure with pronounced peaks associated with liquid clouds at 900 and 700 hPa and with ice clouds near 150 hPa. The maximum in cloudiness near 700 hPa is not observed in the tropical atmosphere and likely represents too much detrainment from shallow convection, wherein both Nordeng and Tiedtke employ an identical representation of shallow convection. Cloud fraction and condensate amounts are similar across the various configurations, with some evidence of compensating biases. For instance, in comparison with the piControl, Nordeng produces more condensate at 900 hPa but less at 700 hPa, whereas Tiedtke produces more liquid cloud at 700 hPa, but less ice is evident in the upper troposphere. Because of this compensation, the albedo of the RCE simulations is similar to the tropical average (Table 2).

[20] To the extent Tiedtke and Nordeng differ, Nordeng is a better match to piControl especially in regard to the vertical temperature structure, as one would expect because the Nordeng scheme is also used in the piControl simulations. For the most part, the differences are understandable. The more adiabatic updraft model of the Tiedtke scheme produces a warmer and deeper troposphere, which leads to a somewhat elevated peak in the humidity and cloud fraction (respectively cloud ice) profiles. The RCE vertical profile simulated by Nordeng looks, in many respects, more similar to the piControl than it does to the RCE vertical profile simulated by Tiedtke. Moreover, in terms of features that are not immediately attributable to the representation of convection, like the double peak in lower tropospheric cloud fraction, both show behavior consistent with the piControl simulation. Altogether these results suggest that the mean RCE climate of a GCM may be a good predictor of its mean tropical climate when run in a more standard configuration. Learning something about RCE thus stands a chance of advancing understanding of more complex configurations.

3.3. Large-Scale Circulations

[21] A number of studies suggest that the mean RH of the tropical atmosphere depends on the degree of convective aggregation [*Bretherton et al.*, 2005; *Muller and Held*, 2012; *Tobin et al.*, 2012], with more aggregation leading to an on average drier troposphere. The relatively good match between the mean RH in RCE and in the piControl tropics and evidence of persistent large-scale circulations in RCE motivate a closer look at this issue. The relatively long-lived large-scale circulations that develop in the RCE version of ECHAM also provide an opportunity to more critically investigate the regime dependence of clouds, and whether differences between cloudiness in the upwelling and downwelling regions of the piControl climate are similar to what is found in RCE.

[22] Following *Bony et al.* [2004], the probability density function (PDF) of $\overline{\omega}$, $P_{\overline{\omega}}$, is used to define dynamical regimes based on weekly averaged data as defined in section 2.2. This analysis has been repeated for longer and shorter timescales, which leads to a narrowing or broadening of $P_{\overline{\omega}}$ as one would expect. Weekly averaged data are used for the reasons discussed in section 2.

[23] Given the differences between the RCE configuration and that used in the piControl simulation, the overall structure of the large-scale circulation in RCE is surprisingly similar to that found over the tropical oceans in the piControl simulation. This point is illustrated by comparing $P_{\overline{\omega}}$ for the different simulations, as shown in Figure 5. All three experiments are negatively skewed with the highest statistical weight of Tiedtke and piControl at 25 hPa d^{-1} and Nordeng at 30 hPa d^{-1} and a threefold similarly long tail toward strong ascending velocities. The similarity in the value at which $P_{\overline{\omega}}$ maximizes is perhaps not that surprising, as it is determined by the ratio of the clear-sky cooling rate to the lapse rate of dry static energy. The more stable lapse

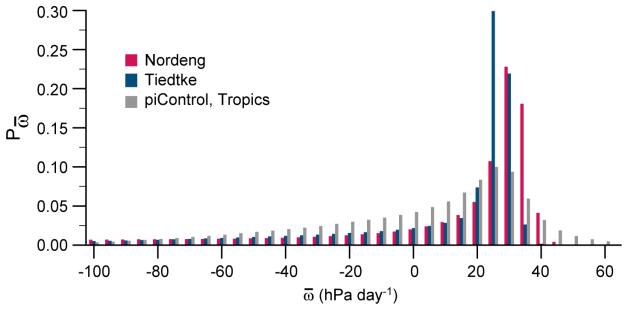

Figure 5. PDF of the mass-weighted vertically averaged velocity $P_{\overline{\omega}}$ of the RCE model with the Nordeng and Tiedtke convection scheme, using weekly averaged data. 20 years of monthly means are used for the piControl values, considering only tropical ocean grid points. The data are binned by 5 hPa d^{-1}. The effect of the different timescales is discussed in section 2.2.

rate in the Tiedtke RCE simulations is consistent with $P_{\overline{\omega}}$ peaking at a somewhat less positive value of $\overline{\omega}$. Nordeng produces a somewhat broader distribution of $P_{\overline{\omega}}$ as compared with Tiedtke, but both lack the strong downwelling regions associated with the cold ocean boundary-current regions in the piControl climate. Moreover, both tend to have substantially less, almost half as much, weak upwelling motions. As a result, the mean upward motion is considerably stronger, almost double in the RCE configurations (Table 3), and the intensity of the circulation, as measured by the difference between the mean upward and downward motion, is stronger in RCE.

[24] Given the differences of a factor two, it might seem curious to claim that the overturning circulation in the RCE simulations is similar to that in piControl. However, *Bony et al.* [2004] conducted an analog comparison of P_ω using vertical velocities from tropical regions from three GCMs (their Figure 5 compares P_ω for the European Centre for Medium-Range Weather Forecasts, Reading, England, Laboratoire de Météorologie Dynamique, Palaiseau, France, and UK Met Office models). They found disparities in the strength of moderate ascending motion, as well as the value and probability of the most frequent subsiding motion, similar to what is presented in Figure 5. Or put another way, differences in the tropical overturning circulation as represented by disparate GCMs simulating the present climate are of the same magnitude as the differences in the overturning circulations of the RCE versus the piControl climate simulated by ECHAM6.

Table 3. Mean Vertical Velocity Values of Ascending Air ($\overline{\overline{\omega} < 0.0}$), Descending Air ($\overline{\overline{\omega} \geq 0.0}$), and Total Air Masses ($\overline{\overline{\omega}}$)[a]

Experiment	$\overline{\overline{\omega} \geq 0.0}$	$\overline{\overline{\omega} < 0.0}$	$\overline{\overline{\omega}}$
Nordeng	27.5	−70.6	0.0
Tiedtke	24.3	−62.3	0.0
piControl, ocean tropics	24.2	−36.7	0.6

[a]All values are given in hPa d^{-1}.

[25] RCE also captures the differences between the structure of the downwelling and upwelling tropical atmosphere in piControl (Figure 6, top and bottom, respectively). This includes the tendency of the upwelling regions to be moister at all levels, but particularly in the middle troposphere. The absence of high clouds in the downwelling regions, and differences in condensate loading between the upwelling and downwelling regimes in the piControl are well represented by both Tiedtke and Nordeng.

[26] From the perspective of climate, a more crucial test is how cloud radiative effects (CREs) depend on the details of the large-scale circulation. To address this question, CRE is conditioned on vertical motion for Nordeng, Tiedtke, and piControl and plotted in Figure 7. The similarities between Nordeng and piControl are striking. For all values of $\overline{\omega} < 20$ hPa d^{-1}, the two simulations are indistinguishable and differ markedly from Tiedtke, suggesting that these effects are more sensitive to the choice of convective scheme than they are to the particular configuration of the tropical climate. This point of view is reinforced by the analysis of *Bony et al.* [2004, Figure 7], which shows differences in CRE between models of the present climate similar to those between Nordeng and Tiedtke. Although the differences in the longwave CRE for Tiedtke versus Nordeng may partially be explained by the somewhat warmer and deeper troposphere simulated by Tiedtke, this cannot explain the differences in the shortwave (SW) CRE. The stronger longwave (LW) CRE and the less negative SW CRE are consistent with the warmer climate simulated by Tiedtke as compared with Nordeng. Only for strong subsidence, where models anyway show less consistent behavior when conditioned on $\overline{\omega}$ [e.g., *Bony and Dufresne*, 2005], do we see that Nordeng and Tiedtke begin to behave more similarly to each other than they do to piControl. These differences tend to be most pronounced for the SW CRE (Figure 7, bottom). This suggests that the low-cloud regimes are more sensitive to the configuration of the large-scale circulation and perhaps somewhat less sensitive to the representation of deep convection, except insofar as it determines the circulation.

[27] In summary, the RCE configuration of ECHAM6 coupled to a mixed-layer ocean produces an atmospheric state that is, in many respects, similar to the tropical atmosphere simulated by an Earth-like configuration of the same model. The overturning circulation of the tropical atmosphere is also similar to that produced by the RCE model and conditionally averaged cloud fields, and CREs particularly in upwelling or weakly downwelling regions are also very similar in the RCE and Earth-like tropical atmosphere. In many statistics, ranging from the tropical thermal structure to the dependence of CREs on $\overline{\omega}$, RCE simulated with convection represented by the Nordeng scheme looks more similar to the Earth's tropical atmosphere, than it does to RCE simulated using the same model but coupled to the Tiedtke scheme. The RCE model samples perhaps a narrower range of circulation regimes but encapsulates many of the features of the full circulation; given the simplicity it engenders, it appears worthwhile to more deeply understand.

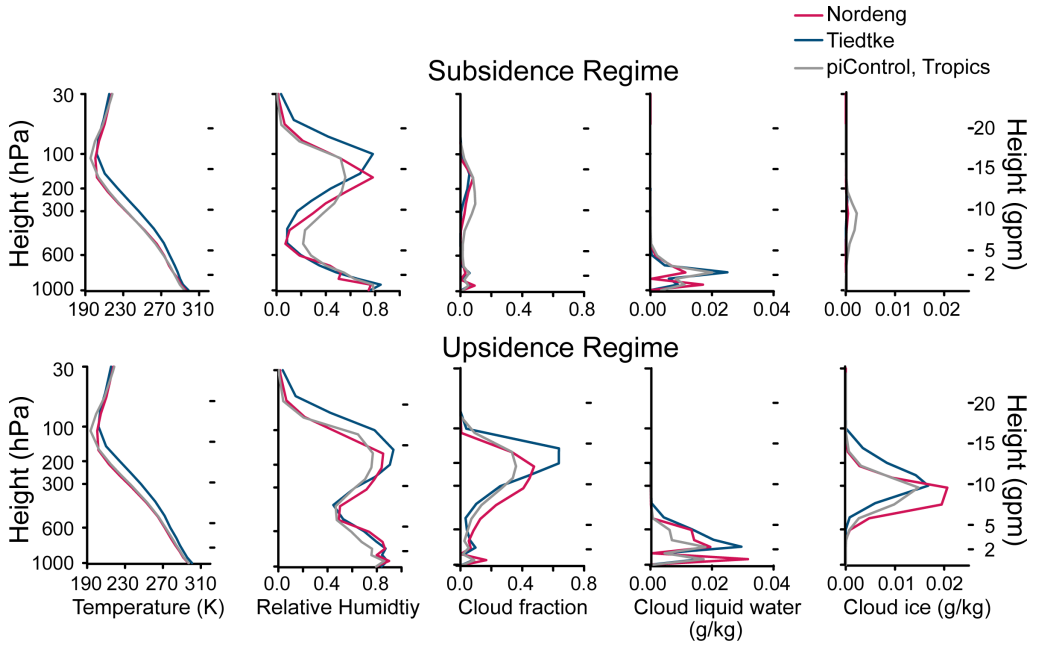

Figure 6. Dynamically sampled vertical profiles of mean temperature, RH, cloud fraction, cloud liquid water, and cloud ice. The weekly data are sampled into subsidence regime, where $\overline{\omega} \geq 0.0$ hPa d^{-1}, and upsidence regime, where $\overline{\omega} < 0.0$ hPa d^{-1}.

4. Climate Change in RCE

[28] To investigate the behavior of the RCE model in a changing climate, idealized abrupt fourfold CO_2 and quarter-fold CO_2 experiments were performed. When combined with the preindustrial experiments, whose behavior was described in the last section, one arrives at a total of six experiments as described in Table 1. These six experiments allow for the definition of four climate change experiments in which CO_2 is changed by a factor of 4, two climate change experiments for each convection scheme. With the help of these four climate change experiments, two main points are discussed: the climate sensitivity and feedbacks in the RCE model. An enduring question is how sensitive the climate sensitivity and the feedbacks are to the particular atmospheric configuration.

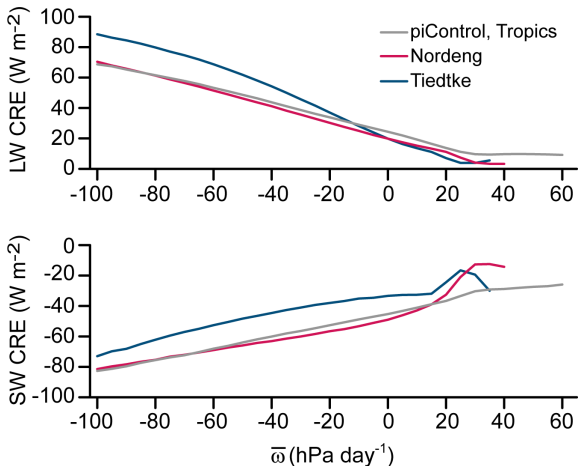

Figure 7. Longwave and shortwave CRE as a function of the vertical velocity that is vertically mass-weighted averaged from 925 to 200 hPa. Weekly averaged data of 3 years in equilibrium are used for the RCE Nordeng and Tiedtke values, whereas 20 years of monthly means are used for the piControl analysis, considering only tropical ocean grid points.

[29] The equilibrium climate sensitivity, $\Delta T_{2\times}$, estimated from the four RCE climate change experiments ranges from 1.4 to 2.0 K. These values are about half as large as for ECHAM6 run in a standard configuration, for which $\Delta T_{2\times} = 3.4$ K. Because the experiments are for a CO_2 quadrupling, $\Delta T_{2\times}$ is calculated as follows:

$$\Delta T_{2\times} = \frac{1}{2}\Delta T_{4\times}, \tag{4}$$

where $\Delta T_{4\times}$ is the change in the globally averaged surface temperature, in stationarity, between pairs of simulations with a factor of 4 difference in the atmospheric CO_2 concentration. $\Delta T_{2\times}$ thus measures the surface temperature change that would be expected for a doubling of atmospheric CO_2 and defines the classical equilibrium climate sensitivity [e.g., *Charney et al.*, 1979]. $\Delta T_{2\times}$ shows some dependency on temperature and the chosen convection scheme (Figure 8).

[30] For reference, Figure 8 also presents the $\Delta T_{2\times}$ estimated from a full ECHAM6, coupled to a mixed-layer ocean (ECHAM6-MLO), simulation, both for the globe as a whole and for the tropical ocean. The value derived only from changes of the tropical oceans is 2.6 K, roughly intermediate between the value for the full model

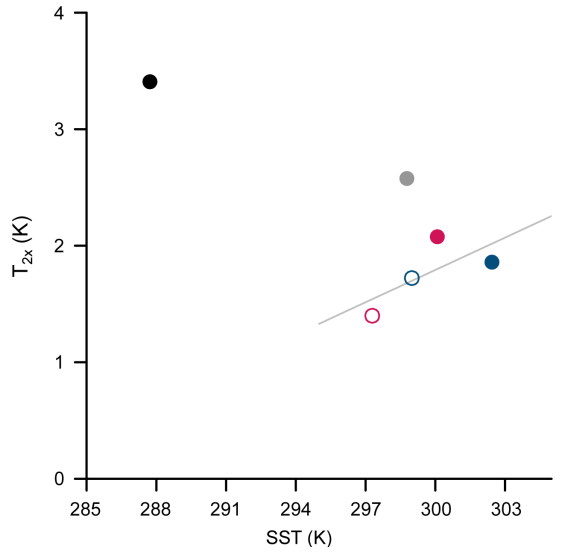

Figure 8. Climate sensitivities corresponding to a 2× CO_2 increase. Values of an abrupt fourfold CO_2 to two steady states, quarter-fold CO_2 (open circles), and one-fold CO_2 (filled circles) for the RCE model with the Nordeng and Tiedtke convection scheme in blue and pink, respectively, are shown. Values to a fourfold CO_2 increase are divided by two to conform to the common definition of climate sensitivity. The climate sensitivity of a fourfold CO_2 increase to preindustrial CO_2 concentration for the common ECHAM6 setup with an underlying mixed-layer ocean is shown for the whole globe (black dot) and for the tropics over the ocean (gray dot).

and the estimates from the RCE calculations, but consistent with a tendency for a much lower climate sensitivity in RCE. If one assumes that the tropical oceans warm more in the standard configuration than in RCE, simply because the continents as well as the extratropics through polar amplification warm so much more, and that some of this warming is felt by the tropical ocean, it suggests that between a third and one half of the warming from a doubling of atmospheric CO_2 can be attributed to extratropical processes or land-sea interactions.

[31] The comparably low-climate sensitivities of the RCE model used here are consistent with the finding of $\Delta T_{2\times}$ in RCE models in *Ramanathan and Coakley* [1978], ranging from 1.45 to 1.90 K. However, the values that they report are based on simple RCE models, which neglect a number of important feedback mechanisms including those associated with clouds and changing lapse rates. The expectation that high clouds will keep the same cloud-top temperature in a warming climate, following what has come to be known as the fixed anvil temperature (FAT) hypothesis [*Hartmann and Larson*, 2002], has emerged as an important positive cloud feedback that is robust in GCM studies. When this feedback is included in the simple RCE models, $\Delta T_{2\times}$ is shown to increase by more than 1 K [*Augustsson and Ramanathan*, 1977] and becomes similar to the range of $\Delta T_{2\times}$ (2.1–4.4 K) reported for the CMIP3 models (Randall et al., 2007, Table 8.3). Unlike the simple RCE models, Nordeng and Tiedtke include the same fully interactive representation of clouds, humidity, and temperature that are used in the full CMIP3 and CMIP5 models. Among the major feedback mechanisms, only surface albedo feedbacks are missing, but experiments with the full ECHAM suggest that these can only explain a small part, about 0.2 K, of the difference (T. Mauritsen et al., Climate feedback efficiency and synergy, submitted to *Climate Dynamics*, 1–22, 2012). This raises the question as to whether the smaller climate sensitivity in RCE is found, because the FAT hypothesis may not be captured in the RCE configuration of ECHAM6 or, for some other reason, for instance changes in the water vapor or low-cloud feedbacks.

[32] The lower climate sensitivity of ECHAM6 in RCE does not appear to result from a missing longwave feedback from high clouds. This is demonstrated by comparing the brightness temperature (T_B) from the OLR of the 25% strongest convecting regions, assuming that those regions will most likely contain anvil cloud tops. Figure 9 shows T_B as a function of the surface temperature in the same grid column for the full suite of six RCE simulations, as well as for the tropical oceans of the piControl experiment. As anticipated, T_B remains approximately constant, as surface temperatures warm. The observed range of brightness temperatures in the RCE simulations is less than 1 K without considering the one Tiedtke outlier at T_B = 244.5 K. Even when including this data point into the range of RCE simulations, the range of brightness temperatures is only about 4.5 K, being of a similar magnitude as the range given by *Hartmann and Larson* [2002], and small as compared to the total range of brightness temperatures, 50 K

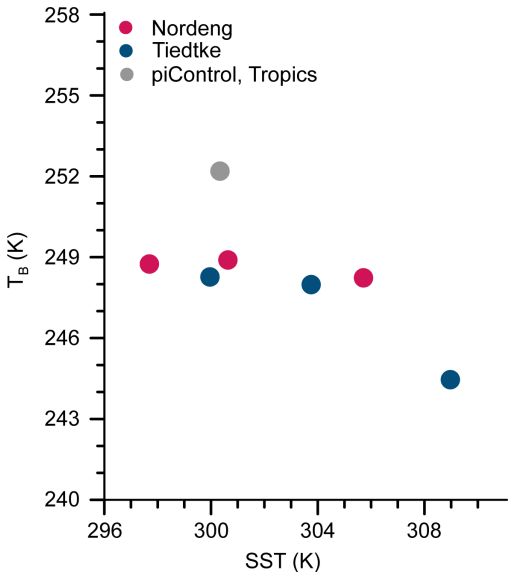

Figure 9. Test of the FAT hypothesis with the brightness temperature, T_B (K) as a function of mean SST (K). Only values from the 25% strongest convecting areas are included for the analysis. Sampled means of weekly averaged data of the RCE model and monthly averaged data of the piControl, only using tropical grid points over ocean, are shown.

across the RCE experiments. T_B from the piControl is also similar to the estimates from RCE. The brightness temperatures shown in Figure 9 are higher than the expected air temperature at the top of high clouds of about 227 K [e.g., *Zelinka and Hartmann*, 2010], which suggests that the clouds are not completely opaque at the top of the convecting regions. Nevertheless, Figure 9 indicates that the assumption of a FAT is a good one for the RCE models we explore. If anything, there is a slight decrease of T_B with increasing surface temperature, which would constitute a stronger positive climate feedback, as the atmosphere would even be less able to efficiently radiate away the heat as surface temperatures warm.

[33] There is some evidence that feedbacks associated with low clouds, which prevail in the regions of downwelling, are less positive or even negative in RCE with ECHAM6. This would be consistent with the lower $\Delta T_{2\times}$ in RCE. Figure 10 shows the change in shortwave CREs from the four climate change experiments of ECHAM6 RCE, as well as changes over tropical ocean points in the standard ECHAM6-MLO simulations. Cloud masking effects, which differentiate cloud feedbacks as compared with changes in CREs, are expected to be small (particularly in the net where there is some compensation) in the downwelling zones over the ocean in the tropics [*Wyant et al.*, 2012, Figure 1]. Hence, tropical low-cloud feedbacks are substantially weaker (Nordeng) or even negative (Tiedtke) in RCE.

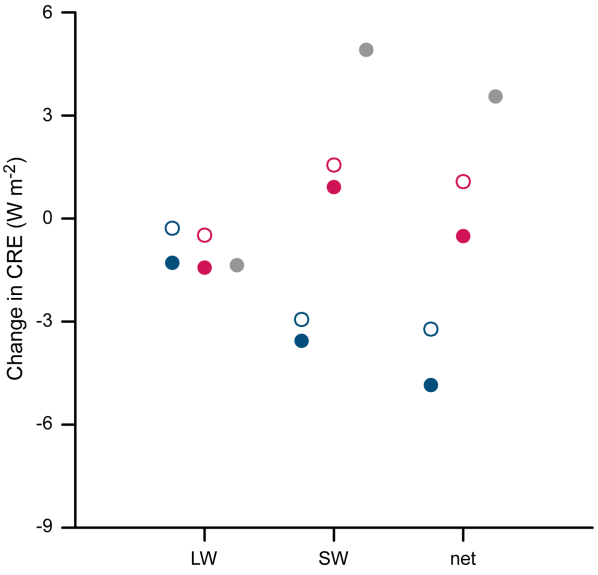

Figure 10. Change in longwave, shortwave, and net CRE in subsiding areas. Open circles show the change in CRE from quarter-fold CO_2 to onefold CO_2 concentration, and filled circles show the change in CRE from onefold CO_2 to fourfold CO_2 concentration. Pink and blue circles represent the values for the RCE model with the Nordeng and Tiedtke convection scheme, respectively, whereas gray circles represent the change in CRE for a common ECHAM6 setup with a mixed-layer ocean, using only tropical grid points over the ocean.

Although we do not account for masking effects, J. Vial et al. (On the interpretation of inter-model spread in CMIP5 climate sensitivity estimates, submitted to *Climate Dynamics*, 2012) show that ΔCRE is a good proxy for the strength of the feedbacks. The sensitivity of the changes in CRE to the choice of convection scheme may be associated with changes in the circulation or differences in the thermodynamic state of the free-troposphere caused by differences in the convection schemes. As shown in Figure 6, Nordeng produces a more pronounced double maximum in the low-level humidity structure, which may precondition cloud changes differently. Both schemes also produce a slowing down of the overturning tropical circulation in a warmer climate, albeit this effect is stronger in Tiedtke. A similar effect, wherein the tropical overturning circulation is found to weaken in response to an increase in atmospheric CO_2 concentrations, is also found in a large number of other models in the tropics (S. Bony et al., Direct effect of carbon dioxide on tropical atmospheric circulation and regional rainfall, submitted to *Nature Geoscience*, 2012).

[34] Although weaker, or even negative, low-cloud feedbacks in the RCE climate change experiments may contribute to the lower climate sensitivity in RCE, they do not explain the respective orderings of the climate sensitivities derived from the four climate change experiments as shown in Figure 8. To explore factors that might influence this ordering of the climate sensitivity, the mean states across the various experiments are compared in Figure 11. A quadrupling of atmospheric CO_2 in RCE has a profound change on the simulated structure of the troposphere, particularly in the upper troposphere, which markedly deepens and warms. The assumption of a constant RH, which is frequently invoked to understand climate change, is relatively well described by the simulations if the change in the tropospheric depth is accounted for, although there is a slight reduction of RH that accompanies warming in the upper middle troposphere (Figure 11c, near 250 hPa) and may also contribute to a smaller $\Delta T_{2\times}$ in RCE compared with the tropics of ECHAM6-MLO.

[35] A closer examination of the mean state suggests that there is a relationship between the depth of the troposphere, or the temperature at 250 hPa, and $\Delta T_{2\times}$. The assumption that the tropical atmosphere follows a moist adiabat leads to the expectation that the change in the temperature in the upper troposphere normalized by $\Delta T_{2\times}$ should be constant, with a value of about 2.7, for the 300 K moist adiabat, and weakly increasing with temperature. In the standard, Earth-like, configuration of ECHAM6, the warming of the upper troposphere follows the moist adiabat associated with the surface warming. Not so for the RCE experiments, where the three experiments with the largest climate sensitivity show superadiabatic warming and one subadiabatic warming, as shown in Figure 12. These experiments suggest that other processes can play a role in determining the temperature of the upper troposphere so that the adiabatic constraint on the temperature in this sensitive part of the atmosphere need not dominate the response in a climate change setting.

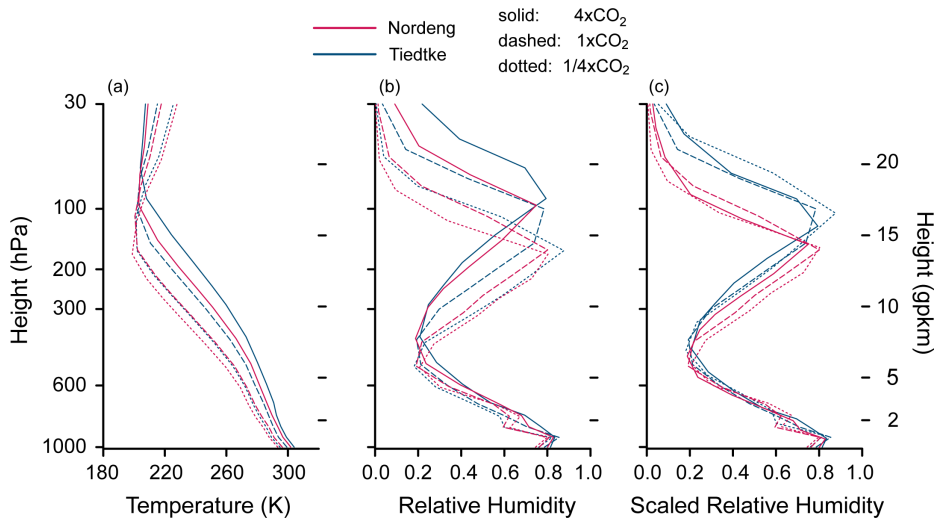

Figure 11. (a) Temperature and (b) RH for the three pairs of RCE experiments. (c) RH with the height axis of the four times and one-quarter times CO_2 experiments rescaled to that of the control experiment within each sample is also shown. The rescaling of the height axis is calculated using the height of the cold point, estimated here from the crossover point of temperature profiles extended downward from the stratosphere and upward from the upper middle troposphere using the mean temperature lapse rate in each region.

[36] Departures from what one would expect if the upper-troposphere temperature followed a moist adiabat depend on the chosen convection scheme and appear to positively correlate with the $\Delta T_{2\times}$. This correlation with the $\Delta T_{2\times}$ is opposite to the negative self-correlation that one would expect given that $\Delta T_{2\times}$ appears in both the dependent and independent variables. Given the smallness of the sample size, only four experiments, it would be imprudent to draw too much from this relationship. However, it merits further investigation, if only because it raises the possibility that models which overestimate the warming in the upper troposphere, relative to a moist adiabat, may also overstate the climate sensitivity.

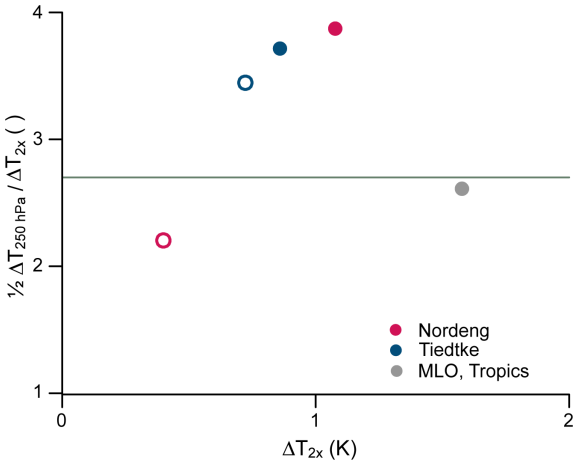

Figure 12. Upper tropospheric temperature changes normalized by $\Delta T_{2\times}$ for the quadrupling experiments plotted as a function of the equilibrium climate sensitivity, $\Delta T_{2\times}$, itself. Open circles show the change from quarter-fold CO_2 to onefold CO_2 concentration, and filled circles show the change in CRE from onefold CO_2 to fourfold CO_2 concentration. Pink and blue circles represent the values for the RCE model with the Nordeng and Tiedtke convection scheme, respectively, whereas gray circles represent the change in CRE for a common ECHAM6 setup with a mixed-layer ocean, using only tropical grid points over the ocean. The gray line represents the 300 K moist adiabat.

5. Conclusions

[37] In an attempt to better understand how Earth's atmosphere responds to changing greenhouse gas concentrations, a version of ECHAM6 has been configured to simulate RCE. The simulations are performed at T63 resolution over the entire Earth surface, but in the absence of either rotation or spatial gradients in insolation, and with a 50 m deep mixed-layer ocean. Three pairs of simulations are carried out at three different atmospheric CO_2 concentrations, one at preindustrial values and one each for a factor of 4 increases or decreases in the concentration. For each CO_2 concentration, two simulations are performed, once with the original formulation of the Tiedtke convection scheme, which tends to have more adiabatic updrafts, and once with the standard ECHAM6 scheme, which is based on Nordeng's modifications.

[38] The simulations are compared to a preindustrial control experiment using the full ESM and are shown to capture the mean state of the tropical atmosphere, over the oceans, with reasonable fidelity. Differences in the energy input in the RCE simulations, which receive a solar irradiance corresponding to the global average, are almost identical to the energy exported by the tropics in the control experiment so that mean temperatures are within 4 K of the control experiment. Significant features of the vertical structure of the tropical atmosphere

are also well reproduced by RCE. This includes the depth of the troposphere, the temperature structure of the atmosphere as a whole, but also a double peaked humidity structure characterized by high near-surface and upper-troposphere humidities, and a mid-troposphere humidity minimum. Profiles of clouds and condensate also mimic those of the control simulations, even insofar as to reproduce idiosyncratic features of the control ECHAM simulation, such as a pronounced double peak in low cloudiness, with one peak at 900 hPa and another near 700 hPa.

[39] The simulations also develop a realistic tropical overturning circulation, as measured by the probability distribution of weekly averaged vertical velocity. Regions of upwelling and downwelling motions can be long-lived and are tied to the development of surface temperature anomalies to which persistent regions of convection are coupled. The control simulation differs in that it includes more regions with weak upward motion and strong downward motion than in RCE, but the differences are shown to be of similar size with differences across models simulating the present-day climate. Sampling the mean state as a function of dynamic regime, defined based on the value of the vertically averaged vertical velocity, further suggests that the mean state in RCE as conditioned on the dynamic regime is also similar to that in the tropics of the control simulation. For instance, RCE as simulated with the Nordeng scheme produces CREs that are almost indistinguishable from the present-day tropics simulated in the control simulation for all but the strongest subsidence regimes. The choice of the convection scheme is shown to influence the simulations, but, in most respects, where the convection scheme has an influence, simulations with Nordeng in RCE are more similar to the simulations from the control simulation, which is also based on Nordeng, than they are to simulations of RCE with the original Tiedtke scheme.

[40] The climate sensitivity of RCE as simulated by ECHAM6 is only half of that of the full model and also lower than the climate sensitivity of just the tropical ocean regions in the full model. The RCE simulations do provide evidence of a positive longwave, high-cloud feedback, following the ideas of a FAT, but the low-cloud feedbacks within the downwelling zones of RCE are substantially weaker than in simulations with the full model and perhaps even negative. To a good approximation, the RH is constant in RCE, particularly when account is taken of changes in the depth of the troposphere that accompanies warming. If anything, there is some evidence of weak drying, in a RH sense, of the upper middle troposphere, accompanying warming in RCE. Temperature changes in the upper troposphere are not well described by changes to the moist adiabat in RCE simulations by ECHAM, are sensitive to the choice of convection scheme, and appear to scale with changes in the equilibrium climate sensitivity.

[41] **Acknowledgments.** Issac Held is thanked for the suggestion to try using our full GCM to explore constraints on the surface energy budget, a suggestion that leads to the present work. Tim Cronin is thanked for pointing out mistakes in the representation of the average diurnal cycle used at an earlier stage of this work. The authors thank Florian Rauser for comments on an earlier version of this manuscript. This research was made possible through the support of the Max Planck Society for the Advancement of Science. Computing resources were provided by the German Climate Computing Center (DKRZ), Hamburg. The research leading to these results has received funding from the European Union, Seventh Framework Program (FP7/2007–2013), under grant agreement 244067.

References

Andrews, T., P. M. Forster, and J. M. Gregory (2009), A surface energy perspective on climate change, *J. Clim.*, *22*, 2557–2570, doi:10.1175/2008JCLI2759.1.

Augustsson, T., and V. Ramanathan (1977), A radiative-convective model study of the CO_2 climate problem, *J. Atmos. Sci.*, *34*(3), 448–451, doi:10.1175/1520-0469(1977)034<0448:ARCMSO>2.0.CO;2.

Bony, S., and J. L. Dufresne (2005), Marine boundary layer clouds at the heart of tropical cloud feedback uncertainties in climate models, *Geophys. Res. Lett.*, *32*, L20806, doi:10.1029/2005GL023851.

Bony, S., J.-L. Dufresne, H. L. Treut, J.-J. Morcrette, and C. Senior (2004), On dynamic and thermodynamic components of cloud changes, *Clim. Dyn.*, *22*, 71–86, doi:10.1007/s00382-003-0369-6.

Bony, S., et al. (2011), Carbon dioxide and climate: perspectives on a scientific assessment, *Tech. Rep.*, World Meteorological Organization: WCRP Open Science Conference.

Bretherton, C. S., P. N. Blossey, and M. Khairoutdinov (2005), An energy-balance analysis of deep convective self-aggregation above uniform SST, *J. Atmos. Sci.*, *62(12)*, 4273–4292, doi:10.1175/JAS3614.1.

Callendar, G. (1938), The artificial production of carbon dioxide and its influence on temperature, *Q. J. R. Meteorol. Soc.*, *64(275)*, 223–240, doi:10.1002/qj.49706427503.

Charney, J. G., et al. (1979), Carbon dioxide and climate: A scientific assessment, *Tech. Rep*., National Academy of Science, Washington, DC.

Crueger, T., B. Stevens, and R. Brokopf (2012), The Madden-Julian oscillation in ECHAM6 and the introduction of an objective MJO score, *J. Clim.*, doi:10.1175/JCLI-D-12-00413.1, inpress.

Grabowski, W. W. (2003), Impact of cloud microphysics on convective–radiative quasi equilibrium revealed by cloud-resolving convection parameterization, *J. Clim.*, *16*(21), 3463–3475, doi:10.1175/1520-0442(2003)016<3463:IOCMOC>2.0.CO;2.

Hartmann, D. L., and K. Larson (2002), An important constraint on tropical cloud—climate feedback, *Geophys. Res. Lett.*, *29*(20), 1–4, doi:10.1029/2002GL015835.

Held, I. M. (2005), The gap between simulation and understanding in climate modeling, *Bull. Am. Meteorol. Soc.*, *86*(11), 1609–1614, doi:10.1175/BAMS-86-11-1609.

Held, I. M., R. S. Hemler, and V. Ramaswamy (1993), Radiative-convective equilibrium with explicit two-dimensional moist convection, *J. Atmos. Sci.*, *50*(23), 3909–3927, doi:10.1175/1520-0469(1993)050<3909:RCEWET>2.0.CO;2.

Held, I. M., M. Zhao, and B. Wyman (2007), Dynamic radiative–convective equilibria using GCM column physics, *J. Atmos. Sci.*, *64(1)*, 228–238, doi:10.1175/JAS3825.11.

Manabe, S., and R. Strickler (1964), Thermal equilibrium of the atmosphere with a convective adjustment, *J. Atmos. Sci.*, *21*, 361–385, doi:10.1175/1520-0469(1964)021<0361:TEOTAW>2.0.CO;2.

Manabe, S., and R. T. Wetherald (1967), Thermal equilibrium of the atmosphere with a given distribution of relative humidity, *J. Atmos. Sci.*, *24*(3), 241–259.

Mauritsen, T., et al. (2012), Tuning the climate of a global model, *J. Adv. Model. Earth Syst.*, *4*, M00A01, doi:10.1029/2012MS000154.

Medeiros, B., B. Stevens, I. M. Held, M. Zhao, D. L. Williamson, J. G. Olson, and C. S. Bretherton (2008), Aquaplanets, climate sensitivity, and low clouds, *J. Clim.*, *21*(19), 4974–4991, doi:10.1175/2008JCLI1995.1.

Muller, C. J., and I. M. Held (2012), Detailed investigation of the self-aggregation of convection in cloud-resolving simulations, *J. Atmos. Sci.*, *69*, 2551–2565, doi:10.1175/JAS-D-11-0257.1.

Muller, C. J., P. A. O'Gorman, and L. E. Back (2011), Intensification of precipitation extremes with warming in a cloud-resolving model, *J. Clim.*, *24*(11), 2784–2800, doi:10.1175/2011JCLI3876.1.

Nordeng, T. E. (1994), Extended versions of the convective parameterization scheme at ECMWF and their impact on the mean and transient activity of the model in the tropics, *Tech. Rep.*, *206*, ECMWF, Reading.

Pauluis, O., and I. Held (2002), Entropy budget of an atmosphere in radiative-convective equilibrium. Part I: Maximum work and frictional dissipation, *J. Atmos. Sci.*, *59*(2), 125–139, doi:10.1175/1520-0469(2002)059<0125:EBOAAI>2.0.CO;2.

Ramanathan, V., and J. Coakley, J. A. (1978), Climate modeling through radiative-convective models, *Rev. Geophys.*, *16*(4), 465–489, doi:10.1029/RG016i004p00465.

Randall, D., et al. (2007), Climate models and their evaluation, in: *Climate Change 2007: The Physical Science Basis. Contribution of Working Group 1 to the Fourth Assessment Report of the Intergovernmental Panel on Climate Change*, edited by S. Solomon et al., pp. 1–74, Cambridge Univ. Press, Cambridge, U. K.

Robe, F., and K. Emanuel (1996), Moist convective scaling: Some inferences from three-dimensional cloud ensemble simulations, *J. Atmos. Sci*, *53*(22), 3265–3275, doi:10.1175/1520-0469(1996)053<3265:MCSSIF>2.0.CO;2.

Romps, D. M. (2011), Response of tropical precipitation to global warming, *J. Atmos. Sci.*, *68*(1), 123–138, doi:10.1175/2010JAS3542.1.

Sugiyama, M., P. Stone, and K. Emanuel (2005), The role of relative humidity in radiative-convective equilibrium, *J. Atmos. Sci.*, *62*(6), 2001–2011, doi:10.1175/JAS3434.1.

Taylor, K. E., R. J. Stouffer, and G. A. Meehl (2012), An overview of CMIP5 and the experiment design, *Bull. Am. Meteorol. Soc.*, *93*(4), 485–498, doi:10.1175/BAMS-D-11-00094.1.

Tiedtke, M. (1989), A comprehensive mass flux scheme for cumulus parameterization in large-scale models, *Mon. Weather Rev.*, *117*(8), 1779–1800, doi:10.1175/1520-0493(1989)117<1779:ACMFSF>2.0.CO;2.

Tobin, I., S. Bony, and R. Roca (2012), Observational evidence for relationships between the degree of aggregation of deep convection, water vapor, surface fluxes, and radiation, *J. Clim.*, *25*, 6885–6904, doi:10.1175/JCLI-D-11-00258.1.

Tompkins, A. M., and G. C. Craig (1998), Radiative-convective equilibrium in a three-dimensional cloud-ensemble model, *Q. J. R. Meteorol. Soc.*, *124*(550), 2073–2097, doi:10.1002/qj.49712455013.

van den Heever, S. C., G. L. Stephens, and N. B. Wood (2011), Aerosol indirect effects on tropical convection characteristics under conditions of radiative–convective equilibrium, *J. Atmos. Sci.*, *68*(4), 699–718, doi:10.1175/2010JAS3603.1.

Wyant, M. C., C. S. Bretherton, P. N. Blossey, and M. Khairoutdinov (2012), Fast cloud adjustment to increasing CO_2 in a superparameterized climate model, *J. Adv. Model. Earth Syst.*, *4*, 1–14.

Zelinka, M. D., and D. L. Hartmann (2010), Why is longwave cloud feedback positive?, *J. Geophys. Res.*, *115*, D16117, doi:10.1029/2010JD013817.

Corresponding author: D. Popke, Max Planck Institute for Meteorology, Bundesstrasse 53, 20146 Hamburg, Germany. (dagmar.popke@zmaw.de)